



Design and environmentally benign synthesis of novel thiophene appended pyrazole analogues as anti-inflammatory and radical scavenging agents: Crystallographic, *in silico* modeling, docking and SAR characterization



Malledevarapura Gurumurthy Prabhudeva^a, Srinivasan Bharath^b, Achutha Dileep Kumar^a, Shivalingegowda Naveen^c, Neratur Krishnappagowda Lokanath^d, Bantaganahalli Ningappa Mylarappa^e, Kariyappa Ajay Kumar^{a,*}

^a Department of Chemistry, Yuvaraja College, University of Mysore, Mysuru 570005, India

^b Center for the Study of Systems Biology, School of Biology, Georgia Institute of Technology, Atlanta, GA 30332, USA

^c Institution of Excellence, University of Mysore, Manasagangotri, Mysuru 570006, India

^d Department of Studies in Physics, University of Mysore, Manasagangotri, Mysuru 570006, India

^e Transplant Surgery Section, Rangos Research Center, University Of Pittsburgh, PA 15201, USA

ARTICLE INFO

Article history:

Received 10 May 2017

Revised 11 June 2017

Accepted 14 June 2017

Available online 16 June 2017

Keywords:

Green synthesis
Anti-inflammatory
Antioxidant
Chalcone
Cyclocondensation
Phase transfer

ABSTRACT

Oxidative-stress induces inflammatory diseases and infections caused by drug-resistant microbial strains are on the rise necessitating the discovery of novel small-molecules for intervention therapy. The current study presents an effective and new green protocol for the synthesis of thiophene-appended pyrazoles through 3 + 2 annulations method. Chalcones **3(a-g)** were prepared from 5-chloro-2-acetylthiophene and aromatic aldehydes by Claisen-Schmidt approach. The reaction of chalcones **3(a-g)** with phenylhydrazine hydrochlorides **4(a-b)** in acetic acid (30%) medium and also with freshly prepared citrus extract medium under reflux conditions produced the thiophene appended pyrazoles **5(a-l)** in moderate yields. Structures of synthesized new pyrazoles were confirmed by spectral studies, elemental analysis and single crystal X-ray diffraction studies. Further, preliminary assessment of the anti-inflammatory properties of the compounds showed that, amongst the series, compounds **5d**, **5e** and **5l** have excellent anti-inflammatory activities. Further, compounds **5c**, **5d**, **5g**, and **5i** exhibited excellent DPPH radical scavenging abilities in comparison with the standard ascorbic acid. Furthermore, using detailed structural modeling and docking efforts, combined with preliminary SAR, we show possible structural and chemical features on both the small-molecules and the protein that might contribute to the binding and inhibition.

© 2017 Elsevier Inc. All rights reserved.

1. Introduction

An interest in discovery, design and synthesis of novel small-molecules with anti-inflammatory effects is propelling research in the wider research community in order to prevent the deleterious effects that free-oxide radicals can inflict upon the human body. The most important aspects in drug design are the affinity of the small-molecule for its target, the specificity of its action, drug metabolism and bioactivation. The need of the hour for the

research community is to design drugs with fewer/no side effects and more advantageous attributes for the small-molecule drug than the existing ones. Occasionally, thiophenes can be deleterious and are considered a structural alert, as they form highly reactive metabolite, thiophene S-oxide. However, Duloxetine, a thiophene containing drug, is a blockbuster antidepressant without any adverse effect associated with formation of RMs [1]. This is because of the judicious conjugation of thiophene moiety with naphthalene, which facilitates the potentiality of employing this functional group for the synthesis of small-molecules with desired biological effect and the concomitant lack of any side-effects.

α , β -Unsaturated carbonyl compounds (chalcones) are the principal precursors for the biosynthesis of flavonoids and isoflavonoids. Chalcones are synthesized by various methods that

Abbreviations: TBAB, tetrabutylammonium bromide; PTC, phase transfer catalyst; SAR, structure-activity relationship.

* Corresponding author.

E-mail address: ajaykumar@ycm.uni-mysore.ac.in (K.A. Kumar).

includes, Suzuki reaction, Wittig reaction, Friedel-Crafts acylation, Aldol condensation, Photo-Fries rearrangement etc. but the most common method employed is the Claisen-Schmidt reaction of aromatic aldehyde with acetophenones [2]. Chalcones are treated as versatile building blocks in organic chemistry for the synthesis of bioactive molecules such as benzothiazepines [3], pyrazolines [4], isoxazolines [5], etc. Chalcones have gained importance due to their simple structures and diverse pharmacological applications. It has to be pointed out that they show therapeutic efficacy in the treatment of various diseases. For instance, these compounds have shown inhibitory effects on chemotaxis, phagocytosis and ROS production in human polymorphonuclear neutrophils (PMNs), which facilitated the development of potential immunomodulators [6]. They have also showed anti-inflammatory [7], tyrosinase inhibitor and anticancer [8], antimicrobial [9], antiproliferative [10], and antioxidant [11] activities.

Conventional organic synthesis involves the use of energy, petrochemical ingredients, catalysts and post-reaction separation, purification, storage, packaging, distribution etc. Green synthesis is an emerging field that endeavors to make organic synthesis efficient and effective by means of less energy consumption, higher yields and lesser wastes. The uses of greener solvents in the chemical synthesis has a major potential in benefitting both the human health and the environment [12,13]. Orange lemon (*Citrus limon*) is a species of small evergreen tree native to Asia. Lemons were the primary commercial source of citric acid before the development of fermentation based processes [14]. This manuscript demonstrates a methodology to employ the extract from *Citrus limon* for green synthesis of thiophene appended pyrazole derivatives, which were synthesized alternatively in acetic acid medium too.

Design and development of an accessible procedure for the synthesis of simple heterocycles with various functionalities is a worthwhile contribution in organic synthesis. The compounds with pyrazole moieties are the most prominent class in active pharmaceutical drugs and agrochemicals in controlling infections, diseases and pests [15]. Pyrazoles remains the choice for anti-inflammatory agents in spite of multiple attempts at exploring alternative scaffolds [16,17]. There are many protocols for the synthesis of pyrazoles we mention a few to mention are, the first report on a base catalyzed reaction of hydrazines with 1,3-dicarbonyl compounds to produce pyrazoles [18], 1,3-dipolar cycloaddition of hydrazones to alkenes [19]. Regioselective synthesis of phosphonylpyrazoles was achieved by the reaction of chalcones with an α -diazo- β -ketophosphonate [20], and via Vilsmeier Haack formylation reaction of hydrazones [21].

Further, it is emphasized here that pyrazoles are ubiquitous scaffolds and are regarded as promising molecules with potential applications in medicinal chemistry. Pyrazoles were known to exhibit anticancer [22], antimicrobial and antioxidant [23], anesthetic [24], and analgesic [25] activities. In view of wide range of synthetic and biological applications of pyrazoles, we herein report for the first time, the synthesis of highly substituted derivatives of pyrazoles and the results of their *in vitro* evaluation for anti-inflammatory activities. The demonstrated green synthesis paves the way for future efforts at synthesizing derivatives of pyrazoles that could find widespread applications in medicinal chemistry.

2. Materials and methods

Melting points were determined by an open capillary tube method and are uncorrected. Purity of the compounds was checked on thin layer chromatography (TLC) plates pre-coated with silica gel using solvent system hexane: ethyl acetate (1:4). The spots were visualized under UV light. ^1H NMR and ^{13}C NMR spectra were recorded on Agilent-NMR 400 MHz and 100 MHz spectrometer

respectively. The solvent CDCl_3 , with TMS as an internal standard, was used to record the spectra. The chemical shifts are expressed in δ ppm. Mass spectra were obtained on ESI/APCI-Hybrid Quadrupole, Synapt G2 HDMS ACQUITY UPLC model spectrometer. Elemental analysis was obtained on a Thermo Finnigan Flash EA 1112 CHN analyzer.

2.1. Extraction of lemon juice

Orange lemons were obtained from the locally grown lemon trees. Lemons were cut and squeezed to get the pulp juice (100 mL) into a beaker. The pulp juice was transferred to a jar and was diluted with water (50 mL). The mixture was well agitated to a fine solution with the help of mechanical stirrer. Then the solution was warmed for 30 min at 45–50 °C and filtered to get fine juice.

2.2. X-ray diffraction analysis

Single crystals of suitable dimensions were chosen carefully for X-ray diffraction studies. The X-ray intensity data were collected at a temperature of 293(2) K on a Bruker Proteum2 CCD diffractometer equipped with an X-ray generator operating at 45 kV and 10 mA, using $\text{CuK}\alpha$ radiation of wavelength 1.54178 Å. Data were collected for 24 frames per set with different settings of ϕ (0° and 90°), keeping the scan width of 0.5°, exposure time of 2 s, the sample to detector distance of 45.10 mm and 2θ value at 46.6°. The complete data sets were processed using *SAINT PLUS* [26]. The structures were solved by direct methods and refined by full-matrix least squares method on F^2 using *SHELXS* and *SHELXL* programs [27]. The geometrical calculations were carried out using the program *PLATON* [28]. The molecular and packing diagrams were generated using the software *MERCURY* [29].

2.3. Pharmacological screening

2.3.1. Anti-inflammatory activity

Inflammation-mediated disorders are on the rise and hence, there is an urgent need for the design and synthesis of new anti-inflammatory drugs with higher affinity and specificity for their potential targets. Keeping this in view, the series of new synthesized pyrazole derivatives were assessed for their potential anti-inflammatory activities. In this study, we have assessed the small molecules for their ability to block the upstream enzyme sPLA₂. This is to ensure that multiple enzyme targets are available for combinatorial drug administration to increase potency and efficacy of blocking the pathway.

2.3.1.1. Purification of sPLA₂ (VRV-PL-8a) from *V. Russellii* venom. sPLA₂ (VRV-PL-8a) from *Vipera russelli* venom was purified to homogeneity by reported procedure [30] and the protein was estimated by Lowry's method [31]. Briefly, *V. russelli* venom (80 mg) was fractionated on pre-equilibrated Sephadex G-75 column (1.5 × 160 cm) using 50 mM phosphate buffer pH 7.0. The protein was resolved into major three peaks. The second peak, constitute about 30% of the total protein, which showed major sPLA₂ activity. This sPLA₂ peak fraction was lyophilized and further subjected to pre-equilibrated CM-Sephadex C-25 column (1.5 × 45 cm) chromatography. The fractions were eluted stepwise using phosphate buffers of varied ionic strength (50–200 mM) and pH (7.0–8.0). They were resolved into two fractions labeled as V and VIII respectively. The above eluted two fractions were similar to V and VIII protein profiles. The lyophilized fraction VIII was next subjected to Sephadex G-50 column (0.75 × 40 cm) chromatography and eluted using 50 mM phosphate buffer pH 7.0 and obtained

peak was checked for sPLA₂ activity. Homogeneity was checked by SDS-PAGE and RP-HPLC.

2.3.1.2. In vitro inhibition of VRV-PL-8a by thiophene-pyrazole conjugates, 5(a-l). In vitro inhibition of sPLA₂ (VRV-PL-8a) by the synthesized pyrazole derivatives, **5(a-l)**, was assessed by known procedure [32]. Briefly, a 50 µl activity buffer containing 50 mM Tris-HCl buffer pH 7.5, 10 mM CaCl₂ and 100 µM substrate stock (1 mM DMPC in methanol containing 2 mM Triton X-100 in Milli-Q water) were added and incubated for 5 min at 37 °C. Activity was initiated by adding 10 ng of sPLA₂ alone or pre incubated with different concentration of thiophene-pyrazole conjugates **5(a-l)** ranging from 0 to 100 µM for 5 min at 37 °C. Reaction mixtures were incubated for 45 min at 37 °C. 50 µl of quenching solution was added at a final concentration of 2 mM NaN₃, 50 µM ANS and 50 mM EGTA, vortexed for 30 s and incubated for 5 min at rt. 2 µL of this solution was pipetted to measure RFU in a Nanodrop ND3300 Ver 2.8 using an excitation UV-LED (370 ± 10 nm) and emission was recorded at 480 nm in dark condition. Enzyme activity was calculated using the equation

$$\Delta RFU = RFU(\text{Control}) - RFU(\text{Test})$$

where ΔRFU is the change in RFU of test (with sPLA₂) with respect to control (without sPLA₂) in the presence of inhibitors. The resultant RFU was compared with the standard LPC curve to determine the sPLA₂ activity in the presence of inhibitors.

2.3.1.3. Effect of substrate and calcium concentration on VRV-PL-8a. The reaction mixture 0.1 ml containing 10 ng of sPLA₂ alone or with IC₅₀ concentration (11.01 µM) of inhibitor (test compounds) in 50 mM Tris-HCl buffer pH 7.5, 10 mM CaCl₂ and 10 µl of varied substrate stock (0–400 µM) was used for sPLA₂ assay to check the effect of substrate in presence of test compounds. 50 µl of quenching solution was added at final concentration of 50 µM ANS, 2 mM NaN₃ and 50 mM EGTA, vortexed for 30 s and incubated for 5 min at RT. 2 µl of this solution was pipetted to measure RFU. Similar set of experiment was conducted, where in reaction mixture containing IC₅₀ concentration of inhibitor (test compounds) in 50 mM Tris-HCl buffer, pH 7.5, 10 ng of sPLA₂, 100 µM substrate and varied concentration of CaCl₂ (0–12 mM). Reaction was terminated and RFU was measured as described above.

2.3.2. DPPH radical scavenging activity

A freshly prepared DPPH solution shows a deep purple color with an absorption maximum at 517 nm. When the purple color changes to yellow, it leads to decreased absorbance. This is because of the antioxidant molecule reducing the DPPH free radical through donation of hydrogen atom. Instantaneous or concomitant decrease in absorbance would be indicative of potent antioxidant activity by the compound. The capacity to scavenge the stable 2, 2-diphenyl-1-picrylhydrazyl (DPPH) free radical was monitored according to the Blois method [33,34].

3. Results

3.1. Synthesis of chalcones, 3(a-g)

To a solution mixture of 5-chloro-2-acetylthiophene, **1** (10 mmole) and aromatic aldehydes, **2(a-g)** (10 mmole) in methyl alcohol, potassium hydroxide solution (40%, 2 mL) was added. Then the solution mixture was stirred at room temperature for 3–4 h. The progress of the reaction was monitored by TLC. After the completion, the reaction mixture was cooled to room temperature and poured into ice cold water. The solids separated were filtered, washed successively with cold hydrochloric acid (5%) and

cold water. The crude solids were recrystallized from methyl alcohol to obtain the compounds **3(a-g)**.

3.1.1. 1-(5-Chlorothiophen-2-yl)-3-phenylprop-2-en-1-one, 3a

Obtained from 5-chloro-2-acetylthiophene, **1** (1.69 g, 10 mmole) and benzaldehyde, **2a** (1.06 g, 10 mmole) in 78% yield, m.p. 144–145 °C; ¹H NMR (CDCl₃, δ ppm): 6.980–7.026 (m, 3H, Ar–H), 7.126 (d, 1H, *J* = 15.8 MHz, CH=), 7.551–7.663 (m, 2H, Ar–H), 7.786–7.798 (m, 2H, Ar–H), 8.112 (d, 1H, *J* = 16.0 MHz, =CH); ¹³C NMR (CDCl₃, δ ppm): 125.89 (1C), 127.37 (1C), 128.08 (1C), 128.60 (1C), 128.69 (1C), 131.58 (1C), 133.07 (1C), 133.44 (1C), 134.09 (1C), 135.67 (1C), 137.71 (1C), 140.40 (1C), 190.06 (1C, C=O). MS *m/z*: 250.01 (M+2, 35), 248.03 (M+, 100); Anal. Calcd. for C₁₃H₉ClOS (%): C, 62.78; H, 3.65. Found: C, 62.66; H, 3.51.

3.1.2. 1-(5-Chlorothiophen-2-yl)-3-(4-fluorophenyl)prop-2-en-1-one, 3b

Obtained from 5-chloro-2-acetylthiophene, **1** (1.69 g, 10 mmole) and 4-fluorobenzaldehyde, **2b** (1.24 g, 10 mmole) in 71% yield, m.p. 133–135 °C; ¹H NMR (CDCl₃, δ ppm): 6.983 (dd, 2H, *J* = 12.0, 3.1 MHz, Ar–H), 7.310 (d, 1H, *J* = 15.9 MHz, CH=), 7.465 (dd, 2H, *J* = 12.3, 2.4 MHz, Ar–H), 7.734–7.921 (m, 2H, Ar–H), 8.095 (d, 1H, *J* = 16.0 MHz, =CH); ¹³C NMR (CDCl₃, δ ppm): 115.60 (1C), 115.66 (1C), 123.85 (1C), 128.96 (1C), 129.82 (1C), 129.94 (1C), 131.41 (1C), 134.95 (1C), 139.88 (1C), 136.62 (1C), 140.20 (1C), 160.61 (1C), 188.41 (1C, C=O). MS *m/z*: 268.00 (M+2, 34), 266.01 (M+, 100); Anal. calcd. for C₁₃H₈ClFOS (%): C, 58.54; H, 3.02; Found: C, 58.44; H, 2.90.

3.1.3. 1-(5-Chlorothiophen-2-yl)-3-(4-chlorophenyl)prop-2-en-1-one, 3c

Obtained from 5-chloro-2-acetylthiophene, **1** (1.69 g, 10 mmole) and 4-chlorobenzaldehyde, **2c** (1.40 g, 10 mmole) in 82% yield, m.p. 119–120 °C; ¹H NMR (CDCl₃, δ ppm): 7.008 (dd, 2H, *J* = 11.8, 3.0 MHz, Ar–H), 7.176 (d, 1H, *J* = 16.1 MHz, CH=), 7.453 (dd, 2H, *J* = 11.0, 2.3 MHz, Ar–H), 7.680–7.814 (m, 2H, Ar–H), 8.120 (d, 1H, *J* = 16.1 MHz, =CH); ¹³C NMR (CDCl₃, δ ppm): 121.38 (1C), 127.80 (1C), 127.86 (1C), 128.36 (1C), 128.44 (1C), 130.10 (1C), 131.86 (1C), 132.40 (1C), 133.50 (1C), 135.96 (1C), 140.33 (1C), 144.22 (1C), 189.10 (1C, C=O). MS *m/z*: 285.96 (M+2, 13), 283.96 (M+2, 66), 281.95 (M+, 100); Anal. calcd. for C₁₃H₈Cl₂OS (%): C, 55.14; H, 2.85; Found: C, 55.03; H, 2.76.

3.1.4. 1-(5-Chlorothiophen-2-yl)-3-(4-methylphenyl)prop-2-en-1-one, 3d

Obtained from 5-chloro-2-acetylthiophene, **1** (1.69 g, 10 mmole) and 4-methylbenzaldehyde, **2d** (1.20 g, 10 mmole) in 74% yield; m.p. 130–132 °C. ¹H NMR (CDCl₃, δ ppm): 2.435 (s, 3H, CH₃), 7.250 (d, 1H, *J* = 9.2 MHz, CH=), 7.268–7.312 (m, 2H, Ar–H), 7.425–7.484 (m, 1H, Ar–H), 7.493 (dd, 1H, *J* = 9.6, 2.0 MHz, Ar–H), 7.621–7.644 (m, 1H, Ar–H), 7.920 (d, 1H, *J* = 8.0 MHz, Ar–H), 8.142 (d, 1H, *J* = 15.2 MHz, =CH); ¹³C NMR (CDCl₃, δ ppm): 21.65 (1C), 125.87 (1C), 126.04 (1C), 127.31 (1C), 128.76 (1C), 129.38 (1C), 131.45 (1C), 133.40 (1C), 134.07 (1C), 135.17 (1C), 135.84 (1C), 140.02 (1C), 143.98 (1C), 189.59 (1C, C=O). MS *m/z*: 264.03 (M+2, 35), 262.02 (M+, 100); Anal. calcd. for C₁₄H₁₁ClOS (%): C, 64.00; H, 4.22; Found: C, 63.82; H, 4.05.

3.1.5. 1-(5-Chlorothiophen-2-yl)-3-(4-methoxyphenyl)prop-2-en-1-one, 3e

Obtained from 5-chloro-2-acetylthiophene, **1** (1.69 g, 10 mmole) and 4-methoxybenzaldehyde, **2e** (1.36 g, 10 mmole) in 80% yield, m.p. 165–167 °C; ¹H NMR (CDCl₃, δ ppm): 3.870 (s, 3H, OCH₃), 6.964 (dd, 2H, *J* = 11.6, 2.8 MHz, Ar–H), 7.228 (d, 1H, *J* = 16.0 MHz, CH=), 7.449 (dd, 2H, *J* = 11.4, 1.2 MHz, Ar–H), 7.612 (d, 1H, *J* = 9.6 MHz, Ar–H), 7.993–8.023 (m, 1H, Ar–H), 8.116 (d,

^1H , $J = 16.0$ MHz, =CH); ^{13}C NMR (CDCl_3 , δ ppm): 55.48 (1C), 113.93 (1C), 125.84 (1C), 125.86 (1C), 127.31 (1C), 130.62 (1C), 130.94 (1C), 131.36 (1C), 133.32 (1C), 134.02 (1C), 135.89 (1C), 139.56 (1C), 163.66 (1C), 188.23 (1C, C=O). MS m/z : 280.02 (M+2, 35), 278.02 (M+, 100); Anal. calcd. for $\text{C}_{14}\text{H}_{11}\text{ClO}_2\text{S}$ (%): C, 60.32; H, 3.98; Found: C, 60.21; H, 3.87.

3.1.6. 1-(5-Chlorothiophen-2-yl)-3-(4-nitrophenyl)prop-2-en-1-one, **3f**

Obtained from 5-chloro-2-acetylthiophene, **1** (1.69 g, 10 mmole) and 4-nitrobenzaldehyde, **2f** (1.51 g, 10 mmole) in 68% yield, m.p. 107–108 °C; ^1H NMR (CDCl_3 , δ ppm): 6.970 (dd, 2H, $J = 11.4$, 2.5 MHz, Ar–H), 7.255 (d, 1H, $J = 15.8$ MHz, CH=), 7.540 (dd, 2H, $J = 11.9$, 2.1 MHz, Ar–H), 7.866–7.948 (m, 2H, Ar–H), 8.144 (d, 1H, $J = 17.7$ MHz, =CH); ^{13}C NMR (CDCl_3 , δ ppm): 119.92 (1C), 124.65 (1C), 125.33 (1C), 127.37 (1C), 127.46 (1C), 129.60 (1C), 131.10 (1C), 131.18 (1C), 134.34 (1C), 135.75 (1C), 140.44 (1C), 146.60 (1C), 189.18 (1C, C=O). MS m/z : 294.06 (M+2, 36), 292.06 (M+, 100); Anal. calcd. for $\text{C}_{13}\text{H}_8\text{ClNO}_3\text{S}$ (%): C, 53.16; H, 2.75; N, 4.77. Found: C, 53.04; H, 2.63; N, 4.70.

3.1.7. 1-(5-Chlorothiophen-2-yl)-3-(4-(dimethylamino)phenyl)prop-2-en-1-one, **3g**

Obtained from 5-chloro-2-acetylthiophene, **1** (1.69 g, 10 mmole) and 4-(dimethylamino)benzaldehyde, **2g** (1.49 g, 10 mmole) in 66% yield; m.p. 143–145 °C. ^1H NMR (CDCl_3 , δ ppm): 3.004 (s, 6H, $\text{N}(\text{CH}_3)_2$), 6.945 (dd, 2H, $J = 11.7$, 2.6 MHz, Ar–H), 7.234 (d, 1H, $J = 16.0$ MHz, CH=), 7.776 (dd, 2H, $J = 11.3$, 2.3 MHz, Ar–H), 7.822–7.905 (m, 2H, Ar–H), 8.133 (d, 1H, $J = 16.1$ MHz, =CH); ^{13}C NMR (CDCl_3 , δ ppm): 40.48 (1C), 40.57 (1C), 114.90 (1C), 114.98 (1C), 123.81 (1C), 128.36 (1C), 129.62 (1C), 129.76 (1C), 130.40 (1C), 133.30 (1C), 134.34 (1C), 135.90 (1C), 140.52 (1C), 152.60 (1C), 187.40 (1C, C=O). MS m/z : 293.05 (M+2, 36), 291.04 (M+, 100); Anal. calcd. for $\text{C}_{15}\text{H}_{14}\text{ClNOS}$ (%): C, 61.74; H, 4.84; N, 4.80. Found: C, 61.60; H, 4.74; N, 4.67.

3.2. General procedure for the synthesis of 1,5-diaryl-3-(5-chlorothiophen-2-yl)-4,5-dihydro-1H-pyrazoles, **5(a-l)**

To a solution mixture of chalcones, **3(a-g)** (10 mmole) and phenylhydrazine hydrochloride, **4(a-b)** (10 mmole) in freshly prepared lemon juice (30 mL), a catalytic amount of tetrabutylammonium bromide (TBAB) (0.001 mol) was added. Then the mixture was refluxed on a water bath for 5–6 h. The progress of the reaction was monitored by TLC. After the completion, the mixture was filtered and the filtrate was poured into crushed ice. The separated solids were filtered and washed successively with 5% NaHCO_3 and water. The crude solids were recrystallized from ethyl alcohol to get target molecules **5(a-l)** in moderate yields.

Alternatively, a solution mixture of chalcones, **3(a-g)** (10 mmole) and phenylhydrazine hydrochloride, **4(a-b)** (10 mmole) in acetic acid (30%) was refluxed for 5–6 h. The progress of the reaction was monitored by TLC. After the completion, the mixture was cooled and poured into a crushed ice. The separated solids were filtered and washed with water. The crude solids were recrystallized from ethyl alcohol to get target molecules **5(a-l)**. The method produced 4–9% of higher yields in comparison to citrus extract mediated method.

3.2.1. 3-(5-Chlorothiophen-2-yl)-1,5-diphenyl-4,5-dihydro-1H-pyrazole **5a**

Obtained from (E)-1-(5-chlorothiophen-2-yl)-3-phenylprop-2-en-1-one, **3a** (2.48 g, 10 mmole) and phenylhydrazine hydrochloride, **4a** (1.44 g, 10 mmole) in 79% yield, m.p. 162–163 °C; ^1H NMR (CDCl_3 , δ ppm): 3.109 (dd, 1H, $J = 6.9$, 16.1 Hz, $\text{C}_4\text{-H}_a$), 3.746 (dd, 1H, $J = 12.5$, 7.0 Hz, $\text{C}_4\text{-H}_b$), 5.235 (dd, 1H, $J = 6.1$, 12.2 Hz,

$\text{C}_5\text{-H}$), 6.722–6.810 (m, 4H, Ar–H), 6.985–7.024 (m, 5H, Ar–H), 7.190–7.232 (m, 3H, Ar–H); ^{13}C NMR (CDCl_3 , δ ppm): 43.68 (1C, C-4), 64.20 (1C, C-5), 111.35 (1C), 113.45 (1C), 120.16 (1C), 125.20 (1C), 125.68 (1C), 126.54 (1C), 128.53 (1C), 129.19 (1C), 129.77 (1C), 129.98 (1C), 131.59 (1C), 134.65 (1C), 135.20 (1C), 137.60 (1C), 138.44 (1C), 142.80 (1C), 145.66 (1C, C-3). MS m/z : 342.03 (M+, 34), 340.02 (M+, 100); Anal. Calcd. for $\text{C}_{19}\text{H}_{15}\text{ClN}_2\text{S}$ (%): C, 67.35; H, 4.46; N, 8.27; Found: C, 67.20; H, 4.35; N, 8.16.

3.2.2. 3-(5-Chlorothiophen-2-yl)-5-(4-fluorophenyl)-1-phenyl-4,5-dihydro-1H-pyrazole **5b**

Obtained from 1-(5-chlorothiophen-2-yl)-3-(4-fluorophenyl)prop-2-en-1-one, **3b** (2.66 g, 10 mmole) and phenylhydrazine hydrochloride, **4a** (1.44 g, 10 mmole) in 61% yield, m.p. 122–124 °C; ^1H NMR (CDCl_3 , δ ppm): 3.066 (dd, 1H, $J = 6.9$, 16.4 Hz, $\text{C}_4\text{-H}_a$), 3.756 (dd, 1H, $J = 12.1$, 7.4 Hz, $\text{C}_4\text{-H}_b$), 5.231 (dd, 1H, $J = 6.6$, 12.9 Hz, $\text{C}_5\text{-H}$), 6.728–6.809 (m, 5H, Ar–H), 6.991–7.045 (m, 4H, Ar–H), 7.196–7.253 (m, 3H, Ar–H); ^{13}C NMR (CDCl_3 , δ ppm): 43.66 (1C, C-4), 64.37 (1C, C-5), 111.25 (1C), 113.53 (1C), 119.14 (1C), 125.27 (1C), 125.37 (1C), 125.70 (1C), 127.94 (1C), 128.68 (1C), 128.72 (1C), 129.30 (1C), 129.84 (1C), 131.61 (1C), 134.74 (1C), 134.92 (1C), 141.40 (1C), 142.96 (1C), 145.23 (1C, C-3). MS (m/z): 358.01 (M+2, 32), 356.00 (M+, 100); Anal. Calcd. for $\text{C}_{19}\text{H}_{14}\text{ClFN}_2\text{S}$ (%): C, 63.95; H, 3.95; N, 7.85; Found: C, 63.86; H, 3.85; N, 7.72.

3.2.3. 1-(3-Chlorophenyl)-3-(5-chlorothiophen-2-yl)-5-(4-fluorophenyl)-4,5-dihydro-1H-pyrazole **5c**

Obtained from 1-(5-chlorothiophen-2-yl)-3-(4-fluorophenyl)prop-2-en-1-one, **3b** (2.66 g, 10 mmole) and 3-chlorophenylhydrazine hydrochloride, **4b** (1.78 g, 10 mmole) in 65% yield, m.p. 115–117 °C; ^1H NMR (CDCl_3 , δ ppm): 3.039 (dd, 1H, $J = 6.8$, 16.8 Hz, $\text{C}_4\text{-H}_a$), 3.770 (dd, 1H, $J = 12.4$, 17.2 Hz, $\text{C}_4\text{-H}_b$), 5.221 (dd, 1H, $J = 6.8$, 12.4 Hz, $\text{C}_5\text{-H}$), 6.703–6.822 (m, 4H, Ar–H), 7.001–7.068 (m, 2H, Ar–H), 7.205–7.248 (m, 4H, Ar–H); ^{13}C NMR (CDCl_3 , δ ppm): 43.67 (1C, C-4), 63.72 (1C, C-5), 111.29 (1C), 113.56 (1C), 115.19 (1C), 115.40 (1C), 116.15 (1C), 116.36 (1C), 119.34 (1C), 125.44 (1C), 127.38 (1C), 127.47 (1C), 127.64 (1C), 129.87 (1C), 128.97 (1C), 134.80 (1C), 137.12 (1C), 142.92 (1C), 145.10 (1C, C-3). MS (m/z): 394.08 (M+4, 11), 392.08 (M+2, 45), 390.98 (M+, 100); Anal. Calcd. for $\text{C}_{19}\text{H}_{13}\text{Cl}_2\text{FN}_2\text{S}$ (%): C, 58.32; H, 3.35; N, 7.16; Found: C, 58.20; H, 3.31; N, 7.05.

3.2.4. 5-(4-Chlorophenyl)-3-(5-chlorothiophen-2-yl)-1-phenyl-4,5-dihydro-1H-pyrazole **5d**

Obtained from 3-(4-chlorophenyl)-1-(5-chlorothiophen-2-yl)prop-2-en-1-one, **3c** (2.81 g, 10 mmole) and phenylhydrazine hydrochloride, **4a** (1.44 g, 10 mmole) in 62% yield, m.p. 120–122 °C; ^1H NMR (CDCl_3 , δ ppm): 3.034 (dd, 1H, $J = 6.8$, 16.8 Hz, $\text{C}_4\text{-H}_a$), 3.767 (dd, 1H, $J = 12.4$, 7.2 Hz, $\text{C}_4\text{-H}_b$), 5.213 (dd, 1H, $J = 6.4$, 12.4 Hz, $\text{C}_5\text{-H}$), 6.700–6.818 (m, 4H, Ar–H), 6.998–7.063 (m, 5H, Ar–H), 7.152–7.245 (m, 2H, Ar–H); ^{13}C NMR (CDCl_3 , δ ppm): 43.77 (1C, C-4), 64.23 (1C, C-5), 111.32 (1C), 113.50 (1C), 119.10 (1C), 125.25 (1C), 125.60 (1C), 126.47 (1C), 128.50 (1C), 129.10 (1C), 129.86 (1C), 129.91 (1C), 131.52 (1C), 134.77 (1C), 135.16 (1C), 137.63 (1C), 138.42 (1C), 142.86 (1C), 145.47 (1C, C-3). MS (m/z): 376.04 (M+4, 10), 374.02 (M+2, 64), 372.03 (M+, 100); Anal. Calcd. for $\text{C}_{19}\text{H}_{14}\text{Cl}_2\text{N}_2\text{S}$ (%): C, 61.13; H, 3.78; N, 7.50; Found: C, 61.04; H, 3.71; N, 7.39.

3.2.5. 1-(3-Chlorophenyl)-5-(4-chlorophenyl)-3-(5-chlorothiophen-2-yl)-4,5-dihydro-1H-pyrazole **5e**

Previously we have reported the synthesis and structure characterization of this compound [35].

3.2.6. 3-(5-Chlorothiophen-2-yl)-1-phenyl-5-(p-tolyl)-4,5-dihydro-1H-pyrazole **5f**

Obtained from 1-(5-chlorothiophen-2-yl)-3-(p-tolyl)prop-2-en-1-one, **3d** (2.62 g, 10 mmole) and phenylhydrazine hydrochloride **4a** (1.44 g, 10 mmole) in 58% yield, m.p. 117–119 °C; ¹H NMR (CDCl₃, δ ppm): 2.314 (s, 3H, CH₃), 3.044 (dd, 1H, J = 6.4, 16.6 Hz, C₄-H_a), 3.786 (dd, 1H, J = 12.8, 7.4 Hz, C₄-H_b), 5.245 (dd, 1H, J = 6.9, 12.0 Hz, C₅-H), 6.716–6.828 (m, 4H, Ar-H), 6.708–7.123 (m, 4H, Ar-H), 7.159–7.237 (m, 3H, Ar-H); ¹³C NMR (CDCl₃, δ ppm): 21.12 (1C, CH₃), 43.70 (1C, C-4), 64.14 (1C, C-5), 111.30 (1C), 113.47 (1C), 119.12 (1C), 125.25 (1C), 125.60 (1C), 126.41 (1C), 128.59 (1C), 129.10 (1C), 129.78 (1C), 129.97 (1C), 131.56 (1C), 134.75 (1C), 135.11 (1C), 137.64 (1C), 138.44 (1C), 142.86 (1C), 145.36 (1C, C-3). MS (*m/z*): 354.04 (M+2, 32), 352.05 (M+, 100); Anal. Calcd. for C₂₀H₁₇ClN₂S (%): C, 68.07; H, 4.86; N, 7.94; Found: C, 68.00; H, 4.75; N, 7.81.

3.2.7. 1-(3-Chlorophenyl)-3-(5-chlorothiophen-2-yl)-5-(p-tolyl)-4,5-dihydro-1H-pyrazole **5g**

Obtained from 1-(5-chlorothiophen-2-yl)-3-(p-tolyl)prop-2-en-1-one, **3d** (2.62 g, 10 mmole) and 3-chlorophenylhydrazine hydrochloride, **4b** (1.79 g, 10 mmole) in 65% yield, m.p. 106–108 °C; ¹H NMR (CDCl₃, δ ppm): 2.310 (s, 3H, CH₃), 3.043 (dd, 1H, J = 6.8, 16.8 Hz, C₄-H_a), 3.749 (dd, 1H, J = 12.4, 16.8 Hz, C₄-H_b), 5.192 (dd, 1H, J = 6.8, 19.2 Hz, C₅-H), 6.699–6.809 (m, 4H, Ar-H), 6.995–7.156 (m, 6H, Ar-H); ¹³C NMR (CDCl₃, δ ppm): 21.06 (1C, CH₃), 43.72 (1C, C-4), 64.18 (1C, C-5), 111.26 (1C), 113.51 (1C), 119.07 (1C), 125.27 (1C), 125.62 (1C), 126.43 (1C), 128.55 (1C), 129.02 (1C), 129.80 (1C), 129.94 (1C), 131.54 (1C), 134.71 (1C), 135.03 (1C), 137.67 (1C), 138.45 (1C), 142.95 (1C), 145.28 (1C, C-3). MS (*m/z*): 394.03 (M+4, 14), 392.03 (M+2, 65), 390.01 (M+, 100); Anal. Calcd. for C₂₀H₁₆Cl₂N₂S (%): C, 62.02; H, 4.16; N, 7.23; Found: C, 61.92; H, 4.05; N, 7.18.

3.2.8. 3-(5-Chlorothiophen-2-yl)-5-(4-methoxyphenyl)-1-phenyl-4,5-dihydro-1H-pyrazole **5h**

Obtained from 1-(5-chlorothiophen-2-yl)-3-(4-methoxyphenyl)prop-2-en-1-one, **3e** (2.78 g, 10 mmole) and phenylhydrazine hydrochloride, **4a** (1.44 g, 10 mmole) in 58% yield, (gummy mass); ¹H NMR (CDCl₃, δ ppm): 3.043 (dd, 1H, J = 7.2, 16.4 Hz, C₄-H_a), 3.755 (dd, 1H, J = 12.4, 7.2 Hz, C₄-H_b), 3.846 (s, 3H, OCH₃), 5.252 (dd, 1H, J = 6.8, 12.8 Hz, C₅-H), 6.734–6.858 (m, 4H, Ar-H), 6.979–7.046 (m, 3H, Ar-H), 7.122–7.243 (m, 4H, Ar-H); ¹³C NMR (CDCl₃, δ ppm): 43.55 (1C, C-4), 55.46 (1C, OCH₃), 64.22 (1C, C-5), 111.33 (1C), 113.60 (1C), 119.56 (1C), 125.12 (1C), 125.74 (1C), 126.45 (1C), 128.63 (1C), 129.05 (1C), 129.60 (1C), 129.94 (1C), 131.53 (1C), 134.66 (1C), 135.30 (1C), 137.65 (1C), 138.36 (1C), 145.54 (1C, C-3), 156.70 (1C). MS (*m/z*): 370.15 (M+2, 30), 369.14 (MH⁺, 100); Anal. Calcd. for C₂₀H₁₇ClN₂OS (%): C, 65.12; H, 4.65; N, 7.59; Found: C, 65.02; H, 4.53; N, 7.49.

3.2.9. 1-(3-Chlorophenyl)-3-(5-chlorothiophen-2-yl)-5-(4-methoxyphenyl)-4,5-dihydro-1H-pyrazole **5i**

Obtained from 1-(5-chlorothiophen-2-yl)-3-(4-methoxyphenyl)prop-2-en-1-one, **3e** (2.78 g, 10 mmole) and 3-chlorophenylhydrazine hydrochloride, **4b** (1.79 g, 10 mmole) in 63% yield, m.p. 128–130 °C; ¹H NMR (CDCl₃, δ ppm): 2.987 (dd, 1H, J = 6.4, 17.6 Hz, C₄-H_a), 3.822 (s, 3H, OCH₃), 3.934 (dd, 1H, J = 12.4, 17.2 Hz, C₄-H_b), 5.584 (dd, 1H, J = 6.4, 12.4 Hz, C₅-H), 6.788–7.064 (m, 5H, Ar-H), 7.083–7.669 (m, 5H, Ar-H); ¹³C NMR (CDCl₃, δ ppm): 43.40 (1C, C-4), 55.54 (1C, OCH₃), 64.35 (1C, C-5), 112.03 (1C), 113.58 (1C), 119.54 (1C), 125.10 (1C), 125.80 (1C), 126.63 (1C), 128.60 (1C), 129.01 (1C), 129.54 (1C), 129.91 (1C), 131.50 (1C), 134.78 (1C), 135.44 (1C), 137.89 (1C), 138.13 (1C), 145.51 (1C, C-3), 156.82 (1C). MS (*m/z*): 406.07 (M+4, 12), 404.07 (M+2, 64), 402.07 (M+, 100); Anal. Calcd. for

C₂₀H₁₆Cl₂N₂OS (%): C, 59.56; H, 4.00; N, 6.95; Found: C, 59.44; H, 3.85; N, 6.88.

3.2.10. 3-(5-Chlorothiophen-2-yl)-5-(4-nitrophenyl)-1-phenyl-4,5-dihydro-1H-pyrazole **5j**

Obtained from 1-(5-chlorothiophen-2-yl)-3-(4-nitrophenyl)prop-2-en-1-one, **3f** (2.93 g, 10 mmole) and phenylhydrazine hydrochloride, **4a** (1.79 g, 10 mmole) in 58% yield (gummy mass); ¹H NMR (CDCl₃, δ ppm): 3.043 (dd, 1H, J = 6.6, 16.8 Hz, C₄-H_a), 3.756 (dd, 1H, J = 12.6, 7.4 Hz, C₄-H_b), 5.233 (dd, 1H, J = 6.6, 12.6 Hz, C₅-H), 6.743–6.838 (m, 4H, Ar-H), 6.978–7.163 (m, 3H, Ar-H), 7.158–7.262 (m, 4H, Ar-H); ¹³C NMR (CDCl₃, δ ppm): 43.38 (1C, C-4), 64.22 (1C, C-5), 112.18 (1C), 113.54 (1C), 119.33 (1C), 124.10 (1C), 125.40 (1C), 126.50 (1C), 128.47 (1C), 129.04 (1C), 129.42 (1C), 129.88 (1C), 131.39 (1C), 134.50 (1C), 135.70 (1C), 137.94 (1C), 138.20 (1C), 145.64 (1C, C-3), 148.76 (1C). MS (*m/z*): 385.04 (M+2, 35), 383.05 (M+, 100); Anal. Calcd. for C₁₉H₁₄ClN₃O₂S (%): C, 59.45; H, 3.68; N, 10.95; Found: C, 59.33; H, 3.60; N, 10.86.

3.2.11. 1-(3-Chlorophenyl)-3-(5-chlorothiophen-2-yl)-5-(4-nitrophenyl)-4,5-dihydro-1H-pyrazole **5k**

Obtained from (E)-1-(5-chlorothiophen-2-yl)-3-(4-nitrophenyl)prop-2-en-1-one, **3f** (2.93 g, 10 mmole) and phenylhydrazine hydrochloride, **4a** (1.44 g, 10 mmole) in 60% yield, m.p. 153–155 °C; ¹H NMR (CDCl₃, δ ppm): 3.045 (dd, 1H, J = 7.2, 16.4 Hz, C₄-H_a), 3.775 (dd, 1H, J = 12.4, 7.4 Hz, C₄-H_b), 5.242 (dd, 1H, J = 6.6, 12.0 Hz, C₅-H), 6.745–6.835 (m, 4H, Ar-H), 6.980–7.072 (m, 3H, Ar-H), 7.175–7.235 (m, 3H, Ar-H); ¹³C NMR (CDCl₃, δ ppm): 43.46 (1C, C-4), 64.20 (1C, C-5), 112.09 (1C), 113.66 (1C), 119.60 (1C), 124.13 (1C), 125.46 (1C), 126.52 (1C), 128.49 (1C), 129.10 (1C), 129.49 (1C), 129.97 (1C), 131.40 (1C), 134.66 (1C), 135.86 (1C), 137.80 (1C), 138.24 (1C), 145.45 (1C, C-3), 148.36 (1C). MS (*m/z*): 421.09 (M+4, 12), 419.08 (M+2, 66), 417.08 (M+, 100); Anal. Calcd. for C₁₉H₁₃Cl₂N₃O₂S (%): C, 54.56; H, 3.06; N, 10.05; Found: C, 54.47; H, 3.01; N, 10.00.

3.2.12. 3-(5-Chlorothiophen-2-yl)-5-(4-dimethylamino)phenyl)-1-phenyl-4,5-dihydro-1H-pyrazole **5l**

Obtained from 1-(5-chlorothiophen-2-yl)-3-(4-(dimethylamino)phenyl)prop-2-en-1-one, **3g** (2.93 g, 10 mmole) and phenylhydrazine hydrochloride, **4a** (1.44 g, 10 mmole) in 60% yield, m.p. 160–162 °C; ¹H NMR (CDCl₃, δ ppm): 2.946 (s, 6H, NCH₃), 3.061 (dd, 1H, J = 6.9, 16.4 Hz, C₄-H_a), 3.756 (dd, 1H, J = 12.8, 6.8 Hz, C₄-H_b), 5.242 (dd, 1H, J = 6.6, 12.8 Hz, C₅-H), 6.735–6.845 (m, 4H, Ar-H), 6.975–7.052 (m, 4H, Ar-H), 7.16–7.267 (m, 3H, Ar-H); ¹³C NMR (CDCl₃, δ ppm): 40.20 (2C, NCH₃), 43.12 (1C, C-4), 64.31 (1C, C-5), 112.10 (1C), 113.60 (1C), 119.88 (1C), 124.90 (1C), 125.73 (1C), 126.64 (1C), 128.55 (1C), 129.14 (1C), 129.47 (1C), 129.90 (1C), 131.49 (1C), 134.67 (1C), 135.92 (1C), 137.84 (1C), 138.10 (1C), 145.66 (1C, C-3), 150.80 (1C). MS (*m/z*): 384.20 (M+2, 33), 382.19 (M+, 100); Anal. Calcd. for C₂₁H₂₀ClN₃S (%): C, 66.04; H, 5.28; N, 11.00; Found: C, 65.90; H, 5.18; N, 10.87.

4. Discussion

4.1. Chemistry

Initially, the intermediate 3-aryl-1-(5-chlorothiophen-2-yl)prop-2-en-1-ones, **3(a-g)**, were synthesized by base catalyzed reaction of 5-chloro-2-acetylthiophene, **1**, with aromatic aldehydes, **2(a-g)** in methyl alcohol. The cyclocondensation reaction of compounds **3(a-g)** with phenylhydrazine hydrochlorides **4(a-b)** in citrus extract medium in the presence of tetrabutylammonium bromide (TBAB) as phase transfer catalyst (PTC) under reflux conditions

produced pyrazole derivatives **5(a-l)** in moderate yields (Fig. 1). ^1H NMR, ^{13}C NMR, mass spectral and elemental analysis provided the structural proof for the compounds, **3(a-g)** and **5(a-l)**. Further, amongst the series, the structure of the compounds, **5c**, **5e**, and **5g** were confirmed by single crystal X-ray diffraction studies.

The reaction of 5-chloro-2-acetylthiophene **1**, and aromatic aldehydes, **2(a-g)**, in the presence of potassium hydroxide produced 3-aryl-1-(5-chlorothiophen-2-yl) prop-2-en-1-ones, **3(a-g)**, in moderate yields. In ^1H NMR spectra, compounds **3(a-g)** showed two doublets with coupling constant values ranging from $J = 15.0$ – 16.5 Hz, indicating the (E)-configuration around the C=C bond. For instance, compound **3e** showed a singlet at δ 3.870 ppm for OCH_3 , a doublet at δ 7.228 ($J = 16.0$ MHz) for $\text{CH}=\text{C}$ adjacent to carbonyl group and a doublet at 8.116 ($J = 16.0$ MHz) =CH protons. Due to para substitution, two ortho and meta protons each of the aromatic ring appeared as doublet of doublets at 6.964 ($J = 11.6$, 2.8 MHz) ppm, and at 7.449 ($J = 11.4$, 1.2 MHz) ppm. Signals appears as a doublet at δ 7.612 ($J = 9.6$ MHz) ppm and multiplet at 7.993–8.023 ppm were due to aromatic protons. Compound, **3e** showed signals δ 55.48, 125.84 and 133.32 ppm for OCH_3 , $\text{CH}=\text{C}$ adjacent to carbonyl group, and =CH carbons. Carbonyl carbon appears at δ 188.23 ppm. Aromatic carbons showed signals at δ 113.93, 125.86, 127.31, 130.62, 130.94, 131.36, 134.02, 135.89, 139.56, and 163.66 ppm. Compound, **3e** showed a base peak at m/z : 278.02 corresponding to its molecular mass and M+2 peak 280.02 with a relative abundance of 35% due to ^{37}Cl isotope.

Indeed, the synthesis of dihydropyrazole derivatives by an acid-catalyzed reaction of α , β -unsaturated carbonyl compounds with phenylhydrazine is well established [36], however the process is not eco-friendly. In search of new potent anti-inflammatory agents, our strategic aim was to adopt an innovative green synthesis for the post transformation of the chalcones to pyrazoles, because of the fact that green protocol is eco-friendly. In this context, we were successful in employing citrus extract medium for the reaction of chalcones **3(a-g)** with phenylhydrazine hydrochlorides **4(a-b)** to get substituted pyrazole derivatives **5(a-l)** in moderate yields, establishing an alternative to the commonly employed acid (HCl, CH_3COOH) catalyzed cyclocondensation reaction.

^1H NMR spectra of compounds **5(a-l)** did not show the signals appearing as doublet for each of the alkenyl protons of chalcones **3(a-g)**, confirming the (3+2) annulations between chalcones and phenylhydrazine hydrochlorides to form pyrazole derivatives **5(a-l)**. Further, the methylene protons of C-4 atom of newly formed

pyrazole ring in compounds **5(a-l)** exhibited typical ABX spin and are of diastereotopic nature. For instance, the $\text{C}_4\text{-H}_a$ proton of **5c** appears as doublet of doublet at δ 3.039 ($J = 6.8$, 16.8 Hz) ppm; whereas, $\text{C}_4\text{-H}_b$ proton appears as doublet of doublet at δ 3.770 ($J = 12.4$, 17.2 Hz) ppm, respectively. Instead of appearing as a triplet, $\text{C}_5\text{-H}$ resonates with both $\text{C}_4\text{-H}_a$ and $\text{C}_4\text{-H}_b$ and appears as doublet of doublet at δ 5.221 ($J = 6.8$, 12.4 Hz) ppm. Array of signals appearing as multiplet in the region δ 6.703–6.822 ppm, δ 7.001–7.068 ppm and δ 7.205–7.248 ppm were unambiguously assigned to thiophene and aromatic ring protons. The $\text{C}_4\text{-H}_a$ proton of **5d** appears as doublet of doublet at δ 3.034 ($J = 6.8$, 16.8 Hz) ppm; whereas, $\text{C}_4\text{-H}_b$ proton appears as doublet of doublet at δ 3.767 ($J = 12.4$, 7.2 Hz), respectively. Instead of appearing as a triplet, $\text{C}_5\text{-H}$ resonates with both $\text{C}_4\text{-H}_a$ and $\text{C}_4\text{-H}_b$ and appears as doublet of doublet at δ 5.213 ($J = 6.4$, 12.4 Hz) ppm. An array of signals appearing as multiplets in the region δ 6.700–6.818 ppm, δ 6.998–7.063 ppm and δ 7.152–7.245 ppm, were unambiguously assigned to thiophene and aromatic ring protons. Amongst the $\text{C}_4\text{-H}_a$, $\text{C}_4\text{-H}_b$ and $\text{C}_5\text{-H}$ protons, $\text{C}_5\text{-H}$ were the most deshielded due to their close proximity to electronegative nitrogen atoms.

Compound **5g** shows a signal at δ 21.06 ppm due to aromatic CH_3 carbon. The C-4, C-5 and C-3 carbons of newly formed pyrazole ring showed signals correspondingly at δ 43.72, 64.18 and 145.28 ppm. The appearance of signals for C-4 at δ 43.72 ppm and C-5 at δ 64.18 ppm confirms that the pyrazole ring is not aromatic, but is of partially reduced dihydropyrazole form. Signals appeared at δ 111.26, 113.51, 119.07, 125.27, 125.62, 126.43, 128.55, 129.02, 129.80, 129.94, 131.54, 134.71, 135.03, 137.67, 138.45, and 142.95 ppm are unambiguously due to aromatic carbons. Synthesized series of compounds, **3(a-g)** and **5(a-l)** show similar and consistent pattern signals in their respective spectra. Further, all compounds showed satisfactory elemental analyses compared with theoretical values, which strongly favor the formation of the designed products. Further, amongst the series, the structures of **5c** and **5g** were confirmed by single crystal X-ray diffraction studies. Also we have reported the structure of compound **5e** confirmed by single crystal X-ray diffraction studies earlier [35].

4.2. Crystallography

Compound 1-(3-chlorophenyl)-3-(5-chlorothiophen-2-yl)-5-(4-fluorophenyl)-4,5-dihydro-1H-pyrazole **5c** (CCDC#: 1530867) was recrystallized from methanol to give pale yellow crystals

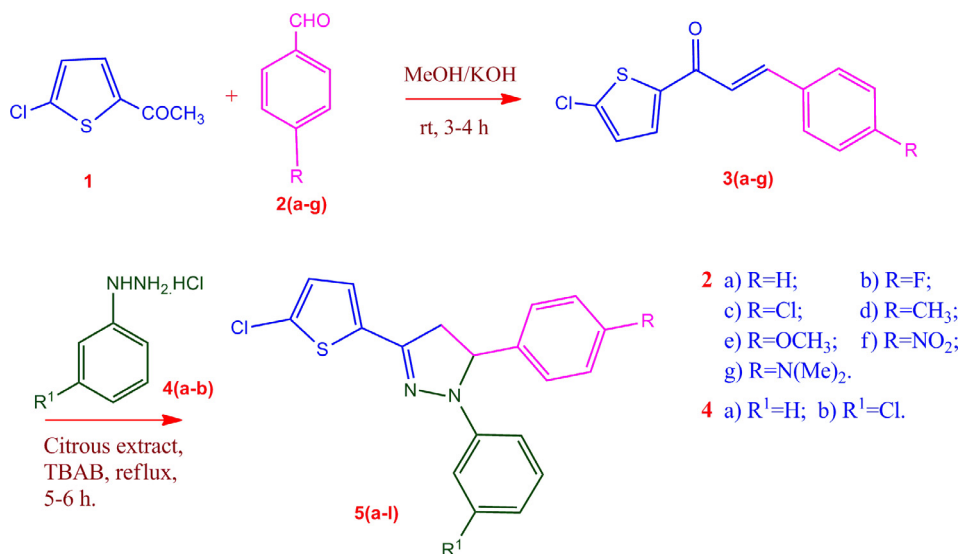


Fig. 1. Schematic diagram for the synthesis of pyrazoles, **5a-l**.

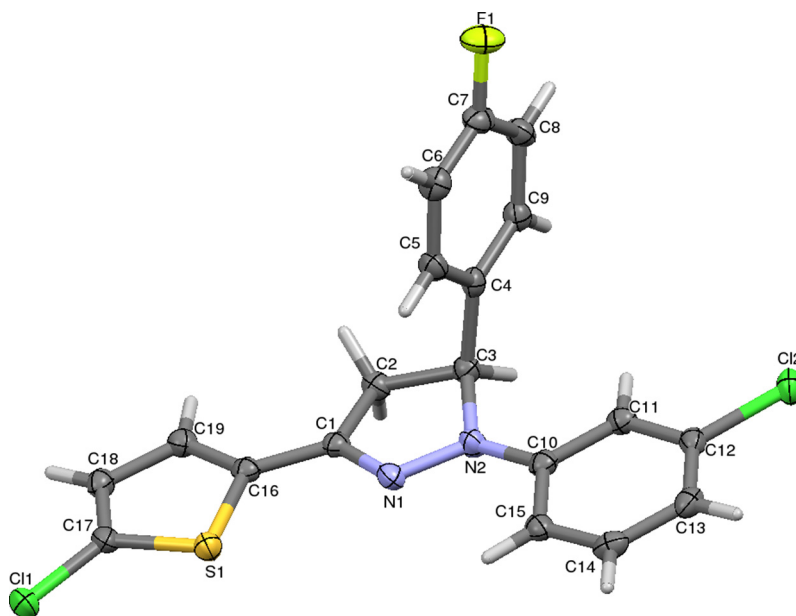


Fig. 2. ORTEP diagram of molecule **5c** with thermal ellipsoids drawn at 50% probability.

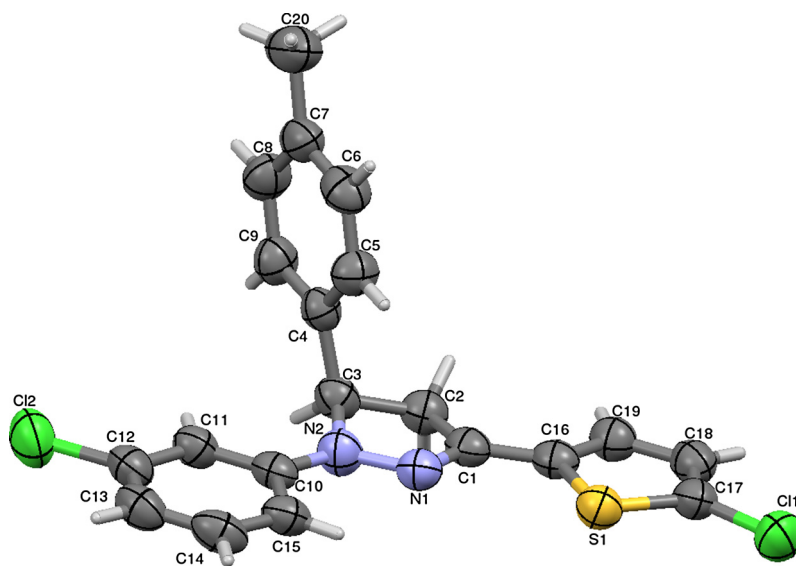


Fig. 3. ORTEP diagram of molecule **5g** with thermal ellipsoids drawn at 50% probability.

suitable for single crystal X-ray diffraction (crystal size $0.28 \times 0.26 \times 0.23$ mm) with the following crystallographic parameters: $a = 18.6646(12)$ Å, $b = 5.5967(4)$ Å, $c = 17.0853(10)$ Å, $\alpha = 90.00^\circ$, $\beta = 107.777(3)^\circ$, $\gamma = 90.00^\circ$, $V = 1699.52(19)$ Å³, $Z = 4$, Goodness-of-fit on $F^2 = 1.063$, R indices (all data) = $R1 = 0.0541$, $wR2 = 0.1523$. The crystal structure of **5c** is monoclinic with a space group of $P 21/c$ and contains pyrazole ring as a central core and has three substitutions viz., 5-chlorothiophen-2-yl, 3-chlorophenyl, and 4-fluorophenyl units. The ORTEP of the molecule with thermal ellipsoids drawn at 50% probability is shown in Fig. 2. Compound 1-(3-chlorophenyl)-3-(5-chlorothiophen-2-yl)-5-(p-tolyl)-4,5-dihydro-1H-pyrazole **5g** (CCDC#: 1530868) was recrystallized from methanol to give pale yellow crystals suitable for single crystal X-ray diffraction (crystal size $0.28 \times 0.25 \times 0.22$ mm) with the following crystallographic parameters: $a = 19.3417(15)$ Å, $b = 5.6555(5)$ Å, $c = 17.5440(14)$ Å, $\alpha = 90.00^\circ$, $\beta = 105.485(4)^\circ$, $\gamma = 90.00^\circ$, $V = 1849.4(3)$ Å³, $Z = 4$, Goodness-of-fit on $F^2 = 1.012$, R

indices (all data) = $R1 = 0.0679$, $wR2 = 0.1879$. The crystal structure of **5g** is monoclinic with a space group of $P 21/c$ and contains pyrazole ring as a central core and has three substitutions viz., 5-chlorothiophen-2-yl, 3-chlorophenyl, and 4-methylphenyl units. The ORTEP of the molecule with thermal ellipsoids drawn at 50% probability is shown in Fig. 3. Complete crystallographic data refinement of compounds, **5c** and **5g** is given in Table 1.

4.3. Anti-inflammatory activity

The results of sPLA₂ inhibition studies of synthesized compounds **5(a-l)** are tabulated in Table 2. The tested pyrazole derivatives, **5(a-l)** inhibited sPLA₂ in dose dependent manner with an IC₅₀ value ranging from 10.106 to 45.463 μM which are computed and analyzed using sigmoidal 4PL curve fit. Amongst the series, **5d**, **5e** and **5i** showed significant inhibition against VRV-PL-8a with IC₅₀ value of 11.0, 10.2, and 10.1 μM respectively (Table 2), compared

Table 1
Crystal data and structure refinement details.

Compound	5c	5g
CCDC Number	1530867	1530868
Empirical formula	C ₁₉ H ₁₃ Cl ₂ FN ₂ S	C ₂₀ H ₁₆ Cl ₂ N ₂ S
Formula weight	391.27	387.31
Temperature	296(2) K	296(2) K
Wavelength	1.54178 Å	1.54178 Å
Refns. for cell determination	2491	2388
θ range for above	4.98°–64.83°	6.30°–64.12°
Crystal system	Monoclinic	Monoclinic
Space group	P21/c	P21/c
Cell dimensions	a = 18.6646(12) Å b = 5.5967(4) Å c = 17.0853(10) Å α = 90.00° β = 107.777(3)° γ = 90.00°	a = 19.3417(15) Å b = 5.6555(5) Å c = 17.5440(14) Å α = 90.00° β = 105.485(4)° γ = 90.00°
Volume	1699.52(19) Å ³	1849.4(3) Å ³
Z	4	4
Density (calculated)	1.529 Mgm ⁻³	1.391 Mgm ⁻³
Absorption coefficient	4.710 mm ⁻¹	4.240 mm ⁻¹
F ₀₀₀	800	800
Crystal size	0.28 × 0.26 × 0.23 mm	0.28 × 0.25 × 0.22 mm
θ range for data collection	4.98°–64.83°	6.30°–64.12°
Index ranges	–21 ≤ h ≤ 21 –6 ≤ k ≤ 6 –19 ≤ l ≤ 19	–22 ≤ h ≤ 22 –4 ≤ k ≤ 6 –20 ≤ l ≤ 20
Reflections collected	11,634	10,441
Independent reflections	2823 [Rint = 0.0586]	3012 [Rint = 0.0523]
Absorption correction	Multi-scan	Multi-scan
Refinement method	Full matrix least-squares on F ²	Full matrix least-squares on F ²
Data/restraints/parameters	2823/0/226	3012/0/228
Goodness-of-fit on F ²	1.063	1.012
Final [I > 2σ(I)]	R1 = 0.0489, wR2 = 0.1467	R1 = 0.0574, wR2 = 0.1748
R indices (all data)	R1 = 0.0541, wR2 = 0.1523	R1 = 0.0679, wR2 = 0.1879
Largest diff. peak and hole	0.396 and –0.430 e Å ⁻³	0.287 and –0.273 e Å ⁻³

Table 2
In vitro anti-inflammatory activity of thiophene appended pyrazole derivatives, **5(a–l)**.^a

Compound	sPLA ₂ IC ₅₀ (μM) ± SEM
5a	19.226 ± 0.182
5b	15.872 ± 0.146
5c	14.340 ± 0.135
5d	11.010 ± 0.109
5e	10.214 ± 0.096
5f	23.440 ± 0.207
5g	22.602 ± 0.214
5h	25.504 ± 0.240
5i	24.626 ± 0.223
5j	45.463 ± 0.394
5k	44.320 ± 0.408
5l	10.106 ± 0.095

^a Results are expressed as mean ± SEM (n = 4).**Table 3**Effect of substrate and calcium concentrations on VRV-PL-8a enzyme inhibition by compounds **5d** (IC₅₀ –11.0 μM), **5e** (IC₅₀ –10.2 μM) and **5l** (IC₅₀ –10.1 μM) with varying calcium concentrations (0–12 mM). The results are expressed as mean ± SEM (n = 4).

CaCl ₂ (mM)	PLA ₂	PLA ₂ - 5d	PLA ₂ - 5e	PLA ₂ - 5l
0	0	0	0	0
1	0.110	0.102	0.058	0.054
2	0.170	0.169	0.087	0.086
4	0.212	0.213	0.108	0.102
6	0.254	0.262	0.130	0.126
8	0.300	0.292	0.149	0.141
10	0.328	0.336	0.156	0.171
12	0.330	0.322	0.173	0.158

Table 4Effect of DMPC concentration (0–400 μM) for VRV-PL-8a activity in presence of compounds **5d** (IC₅₀ –11.010 μM), **5e** (IC₅₀ –10.214 μM) and **5l** (IC₅₀ –10.106 μM). The results are expressed as mean ± SEM (n = 4).

DMPC (mM)	sPLA ₂	sPLA ₂ - 5d	PLA ₂ - 5e	PLA ₂ - 5l
0	0	0	0	0
60	0.630	0.486	0.317	0.246
120	0.942	0.840	0.475	0.416
180	1.173	1.262	0.589	0.611
240	1.285	1.302	0.638	0.654
300	1.422	1.506	0.703	0.748
360	1.649	1.826	0.818	0.586
400	1.652	1.707	0.822	0.849

are expressed as mean ± SEM (n = 4). This study revealed that compounds **5d**, **5e** and **5l** were not competing to the calcium binding site or active site on the VRV-PL-8a enzyme. Inhibition of sPLA₂ by these compounds is independent of calcium concentration and do not chelate calcium ions required for the enzyme activity.

We also studied the effect of compounds **5d** (11.0 μM), **5e** (10.2 μM), and **5l** (10.1 μM) on varying DMPC-substrate concentration (0–400 μM). Their sPLA₂ activity increased with increased substrate concentration (Table 4) suggesting that the binding site of these compounds are organized by substrate binding to VRV-PL-8a.

4.4. DPPH radical scavenging activity

The experiments were performed in triplicate at four different concentrations; the results were taken as a mean ± standard deviation (SD) and are presented in Table 5. Based on the experimental results, we found out those compounds **5j** and **5k** having nitro substitution in the aromatic ring showed lesser antioxidant activities, this might be attributed to strong electron withdrawing nitro group. Compounds **5c**, **5d**, **5g**, and **5i** having fluoro, no, methyl and methoxy substitutions at para positions of the benzene ring exhibited excellent DPPH radical scavenging abilities in comparison with the standard ascorbic acid. Compounds **5a**, **5b**, **5e**, **5f**, **5h**, and **5l** showed moderate radical scavenging activities.

4.5. Preliminary structure-activity relationship

Preliminary SAR (structure activity relationship) analysis was carried out to understand the role of possible functional groups and molecular features that were contributing to increasing inhibition. A total of 38 physicochemical molecular parameters for the 12 compounds reported **5(a–l)**, generated with Joelib and OpenBabel, were assessed pairwise with the potency of the observed Phospholipase A2 inhibition for possible correlation (Fig. 4). The molecular

to other structurally related molecules. To understand the mechanism of action of inhibition, we studied the effect of substrate and calcium concentrations on VRV-PL-8a enzyme inhibition by **5d**, **5e** and **5l**. We examined its inhibition as a function of calcium and substrate concentrations. Compound **5l** at its IC₅₀ concentration (10.1 μM) and with varying calcium (0–12 mM), concentrations, we observed no change in sPLA₂ activity and also did not change the extent of inhibition of **5l**. Similar results were observed with compounds **5d** (11.0 μM) and **5e** (10.2 μM) (Table 3). The results

Table 5
Antioxidant activity of the compounds **5(a-l)** by DPPH radical scavenging method.

Test samples	% Radical Scavenging activity [*]			
	25 (µg/mL)	50 (µg/mL)	75 (µg/mL)	100 (µg/mL)
5a	22.13 ± 0.47	26.90 ± 0.40	29.35 ± 0.55	31.20 ± 0.10
5b	21.25 ± 0.40	24.55 ± 0.35	28.20 ± 0.28	32.45 ± 0.70
5c	14.90 ± 0.40	16.80 ± 0.55	19.90 ± 0.23	21.20 ± 0.50
5d	14.50 ± 0.36	15.10 ± 0.42	18.66 ± 0.60	20.44 ± 0.70
5e	18.40 ± 0.45	21.40 ± 0.80	24.11 ± 0.90	27.60 ± 0.52
5f	23.71 ± 0.46	25.70 ± 0.70	27.40 ± 0.60	30.65 ± 0.90
5g	13.65 ± 0.80	16.84 ± 0.45	20.89 ± 0.70	22.10 ± 0.30
5h	24.45 ± 0.50	27.80 ± 0.52	32.24 ± 0.77	36.13 ± 0.37
5i	15.20 ± 0.46	17.10 ± 0.65	20.35 ± 0.45	23.50 ± 0.45
5j	29.00 ± 0.27	37.28 ± 0.14	42.75 ± 0.26	47.56 ± 0.74
5k	33.35 ± 0.70	38.40 ± 0.84	44.78 ± 0.66	48.02 ± 0.55
5l	24.25 ± 0.50	28.65 ± 0.65	31.10 ± 0.35	37.59 ± 0.41
AA ^a	15.10 ± 0.84	17.85 ± 0.84	21.90 ± 0.55	24.50 ± 0.30

^{*} Values are mean ± SD of three replicates.

^a Ascorbic acid was used as a standard antioxidant.

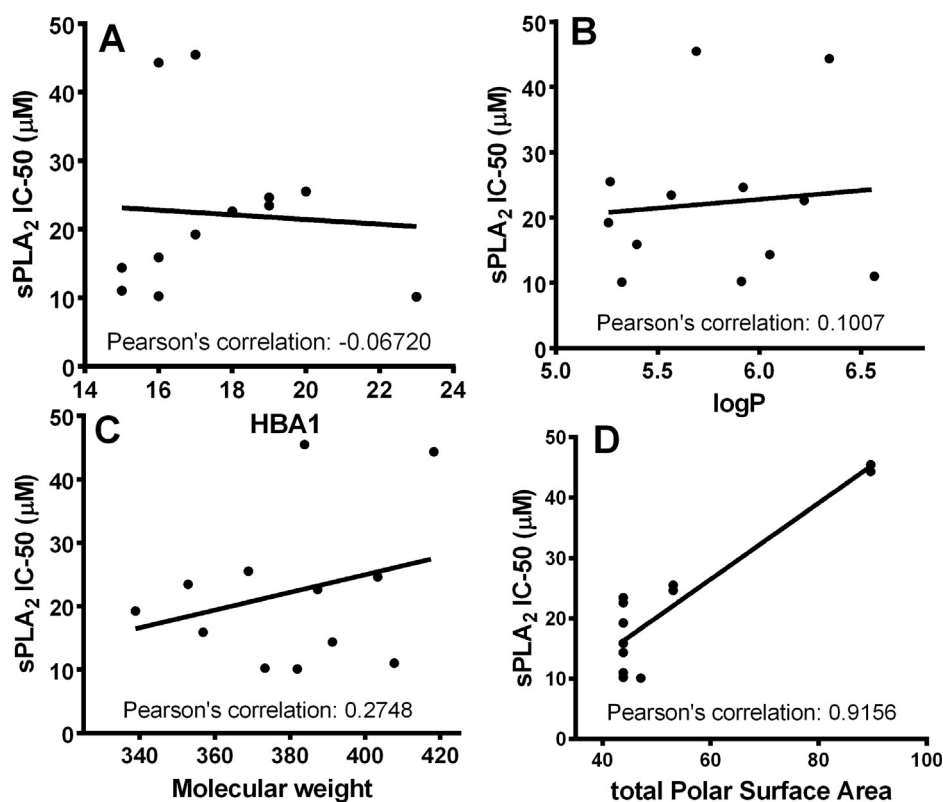


Fig. 4. Pair-wise correlation analysis for four different physicochemical parameters computed for compounds from series **5a-l** against the Phospholipase A2 inhibitory activity. (A) Hydrogen bonding acceptance potential, (B) LogP, (C) Molecular weight and (D) total polar surface area. In the plots, the y-axis represents the IC-50 values for sPLA₂ inhibition and the x-axis indicates the various physicochemical parameters computed for compounds employing Joelib and OpenBabel. The plots were generated in GraphPad Prism, version 4.0 and the linear regression and correlation analysis were carried out using the functions employed by the software. "Pearson's correlation" indicates the correlation coefficient.

parameters included, but were not limited to, variables such as the molecular weight, presence/absence of various halogenated substituents like bromine, chlorine etc, LogP, hydrogen bonding donor/acceptor potential, presence and number of single and double bonds, molecular connectivity parameters like Zagreb group index, shape etc.

The pair-wise comparison shows that, among other parameters, the IC-50 value for sPLA₂ had poor correlations, both positive and negative, with the various parameters assessed. The IC-50 showed poor negative correlation with hydrogen-bonding acceptance

potential and poor positive correlation with parameters like molecular weight and LogP (Fig. 4A–C). However, the correlation was pronounced with Total polar surface area (Fig. 4D) possibly because of the two molecules with stark polar surface area differences. Since the potency of affinity is inversely related with IC-50 values, the data indicates that lesser total polar surface area, lesser molecular weight (to some extent) and lesser LogP (to some extent) contributes towards greater strength of inhibition. On the contrary, more hydrogen bonding potential weakly contributes to the strength of inhibition.

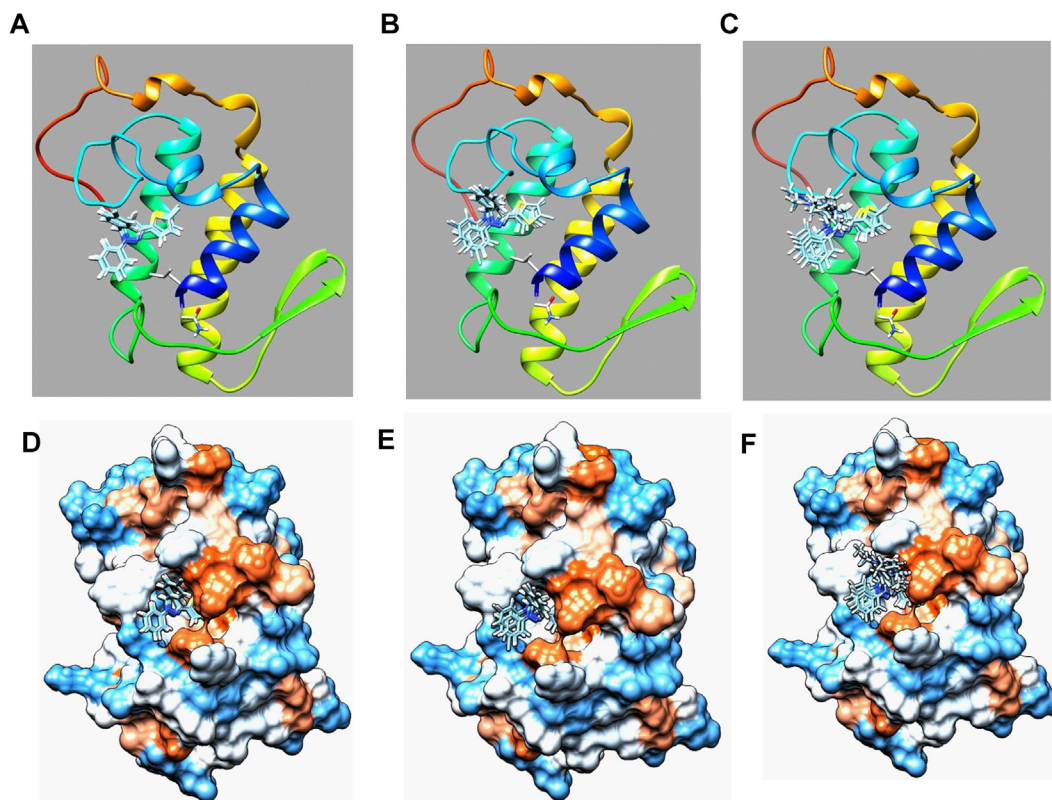


Fig. 5. Molecular modeling of the phospholipase A2 and docking of the small molecule (A) 5d (B) 5e (C) 5l. The Figure shows the ribbon representation of the modelled protein with the overlay of the top 10 docking poses. Surface representation of the protein for the (D) 5d (E) 5e and (F) 5l showing the depth and complementary nature of the docking pocket on the surface. The modeling was performed with Swiss-Model and the docking was done with Swiss-dock. The Figure panels were generated with Chimera 1.11.2.

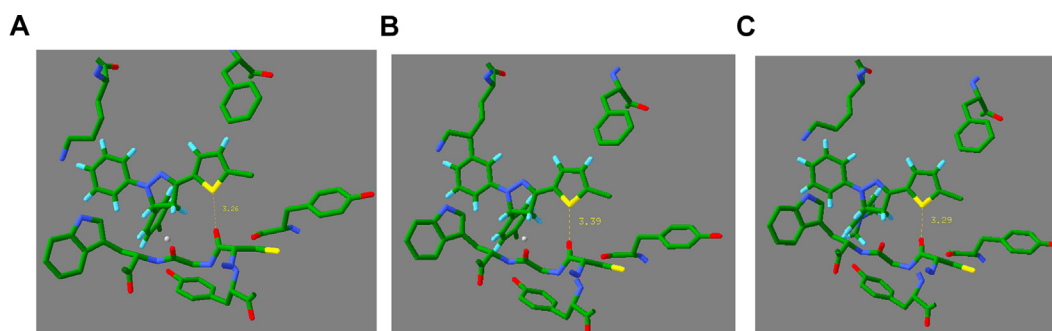


Fig. 6. Representation of residues that are within 3 Å of the docked molecule (A) 5d, (B) 5e and (C) 5l. The calcium molecule is shown as a gray sphere, and the small-molecules and the protein residues are shown in CPK coloration. The docked poses were generated in SWISS-DOCK and the images were generated with Swiss PDB viewer.

4.6. Protein modeling and docking studies

In order to gain insights into the structural aspects of small-molecule binding and assess this inhibition better, the sequence of the human soluble phospholipase A2 (sPLA2) (PDB id: 5G3M) was used as a query in NCBI's pBLAST to search for similar sequences in the *D. russelii* genome. The search picked up the sequence of an acidic phospholipase A2 (A8CG87.1) from *D. russelii* as the closest hit with substantial sequence coverage, 43% sequence identity and a highly significant e-value of $3e-26$. This protein sequence was modelled employing Swiss-model. The best model obtained was a monomer with bound calcium and was modelled on the template 1oz6 with 68.33% sequence coverage and a confident Global model quality estimate (GMQE) of 0.76. This high quality model was used to generate docking poses with the

small-molecules **5d**, **5e** and **5l** that showed the most potent IC₅₀ values for phospholipase A2. The docking was done with SWISS-DOCK in the presence of calcium that contacts residues Y43, G45, G47 and D64. To prepare the small-molecules for docking, explicit hydrogens were added to the small molecules, charges were assigned and the structures were minimized with Chimera. The top most poses belonging to cluster 1 all bind to a highly conserved and deep pocket on the protein's surface. Fig. 5A–C shows the top ten poses of the molecule **5d**, **5e**, and **5l** and Fig. 5D–F shows the surface representation depicting the depth of the pocket accommodating **5d**, **5e** and **5l**. As can be seen from the figure, the top poses of the small-molecules with low binding energies all cluster compactly (<1 Å root mean square deviation) within the predicted docking pocket with **5d** showing the most compact overlap among the top poses followed by **5e** and **5l** in that order.

To understand the nature of residues on the protein contacting the small-molecules and the possible bonds involved in facilitating binding, the residues from the protein that are in proximity (<4 Å cutoff) with the top poses of the bound ligand **5d**, **5e** and **5l**, were highlighted (Fig. 6A–C). As can be seen from the Figure, the small-molecules bind to the highly conserved pocket in close proximity of the calcium binding pocket and are surrounded by a network of aromatic and charged amino acids (Phenylalanine, tryptophan, tyrosine, and arginine) whose sharp turns are supported by flanking glycine residues. The critical hydrogen bond formed by the backbone carbonyl of the glycine to the sulphur atom in the thiophene ring is shown in dotted lines (Fig. 6A–C). However, it has to be pointed out here that the small molecules, though proximal to the calcium in the structure, have a non-overlapping exclusive site of binding. This is in agreement with our experimental results whereby it is shown that the binding of the small-molecules, as assessed by its potency for the receptor, is not proportional to the calcium concentration strongly indicative of independent non-overlapping binding sites. The calcium ion in the structure is coordinated by the backbone carbonyl oxygens of Gly45, Gly47, Tyr43 and the side chain carboxylate group of Asp64.

The structural insights into the sight of binding and the nature of interactions would enable the design of better inhibitors for phospholipase A2 with better geometrical and charge complementarily with the pocket and resultant increase in its affinity and potency.

5. Conclusions

In the present work, we developed a new, environmentally benign, procedure for the direct and one pot synthesis of thiophene-pyrazole conjugates from various thienyl chalcones. The method is a simple and reliable approach towards the synthesis of pyrazoles. The thienyl, N,N-dimethyl and chloro function in a pyrazole ring is posited to be the key feature for the biological potency of the synthesized compounds. Preliminary studies show that compounds **5d**, **5e**, and **5l** possesses excellent anti-inflammatory activities. Further, using detailed structural modeling and docking efforts, combined with preliminary SAR, we show possible structural and chemical features on both the small-molecules and the protein that might contribute to the binding and inhibition.

Conflict of interest

All authors no conflict of interest including financial, personal or other relationships with other people or organizations for this article.

Acknowledgments

The authors are grateful to the IOE Instrumentation Facility, Vijnana Bhavana, University of Mysore, for recording spectra and x-ray diffraction studies.

Appendix A. Supplementary material

Supplementary data associated with this article can be found, in the online version, at <http://dx.doi.org/10.1016/j.bioorg.2017.06.004>.

References

- [1] G. Darja, P.M. Lucija, S.D. Marija, Bioactivation potential of thiophene-containing drugs, *Chem. Res. Toxicol.* 27 (2014) 1344–1358.
- [2] S.N.A. Bukhari, M. Jasamai, I. Jantan, Synthesis and biological evaluation of chalcone derivatives (mini review), *Mini-Rev. Med. Chem.* 12 (2012) 1394–1403.
- [3] M. Manjula, B.C. Manjunath, N. Renuka, K. Ajay Kumar, N.K. Lokanath, 2-(4-Fluorophenyl)-4-(thiophen-2-yl)-2, 3-dihydrobenzo[b][1, 4]thiazepine, *Acta Cryst. E69* (2013). o1608 o1608.
- [4] G.V. Kumar, M. Govindaraju, N. Renuka, B.B.A. Khattoon, B.N. Mylarappa, K.A. Kumar, Synthesis of 1,3,5-triaryl-4,6-dioxo-pyrrolo[3,4-d]-7,8-dihydropyrazoles and their antimicrobial and antioxidant activity, *Rasayan J. Chem.* 5 (2012) 338–342.
- [5] K.A. Kumar, K.M.L. Rai, K.B. Umesha, K.R. Prasad, Synthesis of 3-aryl-5N-aryl-4,6-dioxo-pyrrolo[3,4-d]-7,8-dihydroisoxazoles, *Ind. J. Chem.* 40B (2001) 269–273.
- [6] S.N.A. Bukhari, Y. Tajuddin, V.J. Benedict, K.W. Lam, I. Jantan, J. Jalil, M. Jasamai, Synthesis and evaluation of chalcone derivatives as inhibitors of neutrophils, chemotaxis, phagocytosis and production of reactive oxygen species, *Chem. Biol. Drug Des.* 83 (2014) 198–206.
- [7] S.N.A. Bukhari, X. Zhang, I. Jantan, H.-L. Zhu, M.W. Amjad, V.H. Masand, Synthesis, molecular modeling, and biological evaluation of novel 1, 3-diphenyl-2-propen-1-one based pyrazolines as anti-inflammatory agents, *Chem. Biol. Drug Des.* 85 (2016) 729–742.
- [8] H.-L. Qin, Z.-P. Shang, I. Jantan, O.U. Tan, M.A. Hussain, M. Sher, S.N.A. Bukhari, Molecular docking studies and biological evaluation of chalcone based pyrazolines as tyrosinase inhibitors and potential anticancer agents, *RSC Adv.* 5 (2015) 46330–46338.
- [9] A.K. Kariyappa, N. Shivalingegowda, D.K. Achutha, N.K. Lokanath, Synthesis, crystal and molecular structure, and antimicrobial activity of ethyl 2-(4-methylbenzylidene)-3-oxobutanoate, *Chem. Data Coll.* 3 (2016) 1–7.
- [10] H.-L. Qin, J. Leng, C.-P. Zhang, I. Jantan, M.W. Amjad, M. Sher, M. Naem-ul-Hassan, M.A. Hussain, S.N.A. Bukhari, Synthesis of α,β -unsaturated carbonyl-based compounds, oxime and oxime ether analogs as potential anticancer agents for overcoming cancer multidrug resistance by modulation of efflux pumps in tumor cells, *J. Med. Chem.* 59 (2016) 3549–3561.
- [11] A.D. Kumar, S. Naveen, H.K. Vivek, M. Prabhushwamy, N.K. Lokanath, K. Ajay Kumar, Synthesis, crystal and molecular structure of ethyl 2-(4-chlorobenzylidene)-3-oxobutanoate: Studies on antioxidant, antimicrobial activities and molecular docking, *Chem. Data Coll.* 5 (2016) 36–45.
- [12] P.T. Anastas, J.C. Warner, *Green Chemistry: Theory and Practice*, Oxford University Press, New York, 1998.
- [13] M. Poliakoff, P. Licence, Sustainable technology: green chemistry, *Nature* 450 (2007) 810–812.
- [14] O. Gulsen, M.L. Roose, Lemons: diversity and relationships with selected citrus genotypes as measured with nuclear genome markers, *J. Am. Soc. Hortic. Sci.* 126 (2001) 309–317.
- [15] V. Kumar, K. Kaur, G.K. Gupta, A.K. Sharma, Pyrazole containing natural products: synthetic preview and biological significance, *Eur. J. Med. Chem.* 69 (2013) 735–753.
- [16] Z. Sui, J. Guan, M.P. Ferro, K. McCoy, M.P. Wachter, W.V. Murray, M. Singer, M. Steber, D.M. Ritchie, D.C. Argentieri, 1,3-Diarylcycloalkanopyrazoles and diphenyl hydrazides as selective inhibitors of cyclooxygenase-2, *Bioorg. Med. Chem. Lett.* 10 (2000) 601–604.
- [17] K. Ajay Kumar, M. Govindaraju, Pyrazolines: versatile molecules of synthetic and pharmaceutical applications—a review, *Int. J. ChemTech Res.* 8 (1) (2015) 313–322.
- [18] F.S. Al-Saleh, I.K. Al Khawaja, J.A. Joule, Synthesis of 4-acyl- and 4-alkoxy-carbonylpyrazoles, *J. Chem. Soc., Perkin Trans. 1* (1981) 642–645.
- [19] J. Prabhaskar, V.K. Govindappa, A.K. Kariyappa, Synthesis of 3,4-diaryl-1-phenyl-4,5-dihydro-1H-pyrazole-5-carbonitriles via 1,3-dipolar cycloaddition reactions, *Turk. J. Chem.* 37 (2013) 853–857.
- [20] K. Mohanan, A.R. Martin, L. Toupet, M. Smietana, J.-J. Vasseur, Three-component reaction using the bestmann–ohira reagent: a regioselective synthesis of phosphonyl pyrazole ring, *Angew. Chem. Int. Ed.* 49 (2010) 3196–3199.
- [21] R. Nagamallu, A.K. Kariyappa, Synthesis and biological evaluation of novel formyl-pyrazoles bearing coumarin moiety as potent antimicrobial and antioxidant agents, *Bioorg. Med. Chem. Lett.* 23 (2013) 6406–6409.
- [22] S.R. Stauffer, C.J. Coletta, R. Tedesco, G. Nishiguchi, K. Carlson, J. Sun, B.S. Katzenellenbogen, J.A. Katzenellenbogen, Pyrazole ligands: structure-affinity/activity relationships and estrogen receptor- α -selective agonists, *J. Med. Chem.* 43 (2000). 4934 4934.
- [23] R. Nagamallu, B. Srinivasan, M.B. Ningappa, A.K. Kariyappa, Synthesis of novel coumarin appended bis(formylpyrazole) derivatives: Studies on their antimicrobial and oxidant activities, *Bioorg. Med. Chem. Lett.* 26 (2016) 690–694.
- [24] Z. Christina, D. Florea, D. Constantin, I. Mircea, M. Maria, T. Isabela, M.N. George, Synthesis and biological screening of some 2-(1H-pyrazol-1-yl)-acetamides as lidocaine analogue, *Ind. J. Chem.* 53B (2014) 733–739.
- [25] R. Katoch-Rouse, O.A. Pavlova, T. Caulder, A.F. Hoffmann, A.G. Mukhin, A.G. Horti, Synthesis, structure-activity relationship, and evaluation of SR141716 analogues: development of central cannabinoid receptor ligands with lower lipophilicity, *J. Med. Chem.* 46 (2003) 642–645.
- [26] Bruker, APEX2 and SAINT-Plus, Bruker AXS Inc. Madison, Wisconsin, USA, 2012.
- [27] G.M. Sheldrick, A short history of SHELX, *Acta Cryst.* A64 (2008). 112 112.
- [28] A.L. Spek, PLATON An integrated tool for the analysis of the results of a single crystal structure determination, *Acta Cryst.* A46 (1990). C34 C34.

- [29] C.F. Macrae, I.J. Bruno, J.A. Chisholm, P.R. Edgington, P. McCabe, E. Pidcock, L. Rodriguez-Monge, R. Taylor, J. van de Streek, P.A. Wood, CSD 2.0 - New features for the visualization and investigation of crystal structures, *J. Appl. Cryst.* 41 (2008) 466–470.
- [30] S. Kasturi, T.V. Gowda, Purification and characterization of a major phospholipase A2 from Russell's viper (*Vipera russelli*) venom, *Toxicol. 27* (1989) 229–237.
- [31] O.H. Lowry, N.J. Rosebrough, A.L. Farr, R.J. Randall, Protein measurement with the Folin phenol reagent, *J. Biol. Chem.* 193 (1951) 265–275.
- [32] D.M. Lokeshwari, N.D. Rekha, B. Srinivasan, H.K. Vivek, A.K. Kariyappa, Design, synthesis of novel furan appended benzothiazepine derivatives and *in vitro* biological evaluation as potent VRV-PL-8a and H⁺/K⁺ ATPase inhibitors, *Bioorg. Med. Chem. Lett.* 27 (2017) 3048–3054.
- [33] S. Marsden, Blois, *Nature* 181 (1958) 1199–1200.
- [34] K.R. Raghavendra, N. Renuka, V.H. Kameshwar, B. Srinivasan, K.A. Kumar, S. Shashikanth, Synthesis of lignan conjugate via cyclopropanation: Antimicrobial and antioxidant studies, *Bioorg. Med. Chem. Lett.* 26 (2016) 3621–3625.
- [35] M.G. Prabhudeva, S. Naveen, K.R. Raghavendra, A. Dileep Kumar, Karthik Kumara, N.K. Lokanath, K. Ajay Kumar, 1-(3-Chlorophenyl)-5-(4-chlorophenyl)-3-(5-chlorothiophen-2-yl)-4,5-dihydro-1H-pyrazole, *IUCrData*, 2 (2017) x162048.
- [36] P. Jayaroopa, K. Ajay, Kumar, Synthesis and antimicrobial activity of 4,5-dihydropyrazoline derivatives, *Int. J. Pharm. Pharm. Sci.* 5 (4) (2013) 431–433.